Computational Chemistry

International Edition: DOI: 10.1002/anie.201604552
German Edition: DOI: 10.1002/ange.201604552

Structural Interpretation of Metastable States in Myoglobin–NO

*Maksym Soloviov, Akshaya K. Das, and Markus Meuwly**

Abstract: *Nitric oxide binding and unbinding from myoglobin (Mb) is central to the function of the protein. By using reactive molecular dynamics (MD) simulations, the dynamics following NO dissociation were characterized in both time and space. Ligand rebinding can be described by two processes on the 10 ps and 100 ps timescale, which agrees with recent optical and X-ray absorption experiments. Explicitly including the iron out-of-plane (Fe-oop) coordinate is essential for a meaningful interpretation of the data. The proposed existence of an "Fe-oop/NO-bound" state is confirmed and assigned to NO at a distance of approximately 3 Å away from the iron atom. However, calculated XANES spectra suggest that it is diffcult to distinguish between NO close to the heme-Fe and positions further away in the primary site. Another elusive state, with Fe–ON coordination, was not observed experimentally because it is masked by the energetically more favorable but dissociative ^{4}A state in this region, which makes the Fe–ON local minimum unobservable in wild-type Mb. However, suitable active-site mutations may stabilize this state.*

Characterizing the structure, motions, and functional dynamics of biomolecules is essential for understanding their function. The motions usually involve stable states at their endpoints, which are separated by one or several metastable states (intermediates).[1,2] Experimentally, it is possible to directly and structurally characterize states with sufficiently long lifetimes.[3,4] However, when the lifetime of a state is too short to stabilize only indirect means to infer its existence are available. Optical spectroscopy can reveal the existence of short-lived states through spectral shifts. In Myoglobin (Mb), more direct interrogation of the iron environment is possible with X-ray absorption spectroscopy (XAS)[5] or multidimensional spectroscopy.[6,7] However, associating timescales with particular geometrical arrangements of the involved atoms is usually difficult, except for a few favourable cases.[4] Under such circumstances, computational investigations become a meaningful complement to study the dynamics of the system of interest.

The motion of photodissociated ligands in globular proteins has been studied for a long time. Small molecules that can reversibly bind to the protein active center are ideal, sensitive probes of the interior of such complex systems. Nitric oxide (NO) is a physiologically relevant ligand[8–10] that is involved in modulating blood flow, thrombosis, and neural activity. Experimentally, the binding kinetics of NO to the heme group in myoglobin (Mb) have been studied extensively by time-resolved spectroscopic methods from the UV/Vis to the mid-IR[11–17] region and by resonance Raman[14] techniques. In all cases, the rebinding kinetics are multiexponential, with time constants ranging from the sub-picosecond range to several hundred picoseconds. However, they can be grouped into two general classes: processes on the 10 ps timescale and processes on the 100 ps timescale.[12,14–16,18,19]

Recent experiments have followed the interplay between the Fe out-of-plane (Fe-oop) and the NO ligand motion in a time-resolved fashion.[5,14,16] This work points towards a direct coupling between these two degrees of freedom on the 10 to 100 ps timescale. The structural characterization of these states, however, remained unclear. Furthermore, earlier studies have attempted to characterize the metastable Fe–ON state,[20] and it remains to be determined why this motif that is commonly observed in model compounds[21] is absent in the protein environment despite a stabilization of 5 kcal mol^{-1} or more.[22]

The atomistic dynamics are essential for protein function and provide the basis for the interpretation of the timescales involved at a structural level. Molecular dynamics (MD) simulations are ideal for addressing such questions. In combination with validated energy functions, such simulations can provide the "missing link" between time-resolved experiments and the underlying atomic motions.[4,23,24] For NO interacting with heme in Mb, such potential energy surfaces (PESs) for the bound ^{2}A and ligand-unbound ^{4}A state are available.[25]

Generating a statistically significant number of QM/MM trajectories to analyze and resolve the interplay of the motions involved is beyond current computational methods for systems such as MbNO. For quantitative and meaningful computational investigations, suitable representations that preserve the accuracy of the interpolated PES are used in the simulations. Here, a parameter-free, reproducing kernel Hilbert space (RKHS) based representation, which exactly reproduces the reference data from quantum-chemical calculations, is employed (for details on the PESs, see the Supporting Information).[26,27] RKHS is based on smoothness criteria of the interpolant and has been successfully applied for the study of van der Waals complexes.[28,29]

The present work investigates the reactive dynamics between the ^{4}A and ^{2}A PESs following photodissociation of the NO ligand from the heme iron in Mb. Due to the narrow energy gap between the two states and the existence of two substrates on the ^{2}A PES, interesting dynamics can be expected. By comparison with the experimentally determined rebinding timescales and spectroscopic studies, structural questions related to the molecular dynamics can be addressed.

[*] Dr. M. Soloviov, A. K. Das, Prof. M. Meuwly
Department of Chemistry, University of Basel
Klingelbergstrasse 80, 4056 Basel (Switzerland)
E-mail: m.meuwly@unibas.ch

Supporting information for this article can be found under: http://dx.doi.org/10.1002/anie.201604552.

 © 2016 Wiley-VCH Verlag GmbH & Co. KGaA, Weinheim

To follow the reactive dynamics between the ^{2}A and ^{4}A states, 300 independent simulations were run for a maximum time of 200 ps or until the bound Fe–NO state was formed. Photodissociation was induced by instantaneously switching the force field to the ^{4}A state,[30] which introduces around 50 kcal mol^{-1} of energy into the system,[25] which is comparable with the photon energies used in experiments (49–81 kcal mol^{-1}).[31] The rebinding kinetics are given in Figure 1, which shows the fraction of rebound NO as a function of time. The rebinding kinetics on the sub-nanosecond timescale follow a multiexponential decay with two time constants, $\tau_1 \approx 10$ ps and $\tau_2 \approx 150$ ps, which also depend on the asymptotic separation Δ of the two states (see Table S1 in the Supporting Information). The shift Δ relates the asymptotic energies of the ^{2}A and the ^{4}A PESs for NO at an infinite separation from the heme Fe (see the Supporting Information).

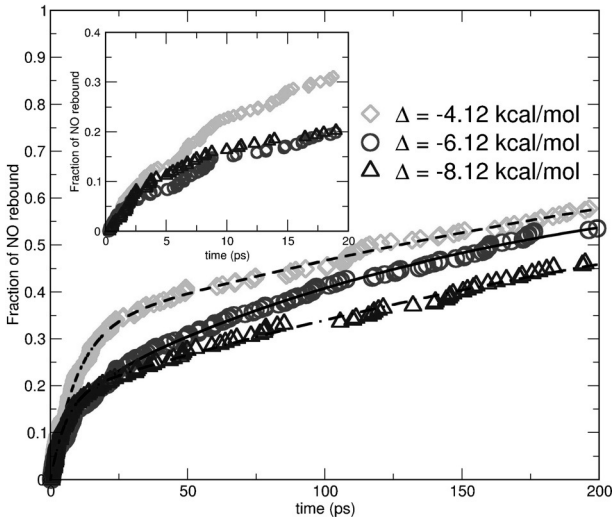

Figure 1. Kinetics and corresponding exponential fits for NO rebinding to the heme Fe after photoexcitation. Simulations were run for three different values of the asymptotic shift Δ.

Typical ligand trajectories are shown in Figure 2. Panel A reports the rebinding on the 1 ps timescale whereas panels B and C represent the rebinding on the timescales τ_1 and τ_2. For τ_1, the ligand only samples the immediate neighborhood of the heme iron center before rebinding. On the 100 ps timescale, rebinding occurs from regions further away. For $\Delta = -6.1$ kcal mol^{-1}, the total numbers of rebinding trajectories are 17 (rebinding within 2 ps), 28 ($2 \le t < 10$), and 115 ($10 \le t < 200$), and 140 rebind on timescales greater than 200 ps, that is, the rebinding efficiency within 200 ps is approximately 55 %. This compares with a rebound fraction of 75 % on the 200 ps timescale as recently determined by XAS measurements.[5]

The simulations described thus far used the PESs fitted to the DFT data and included environmental effects (see the Supporting Information). Corresponding simulations with 200 independent runs on the DFT-only PESs yielded rebinding of 195 trajectories within 200 ps with rebinding times of 2 and 15 ps. This is one order of magnitude faster than for simulations on the refined PESs, which treat the Fe-oop coordinate more accurately and explicitly. This finding is also consistent with previous simulations based on DFT-only PESs.[19,32] Hence explicitly including the Fe-oop motion is essential for quantitative results.

A complementary view of the different rebinding timescales can be gained by analyzing the maximum distance between the Fe center and the ligand during a rebinding simulation. The 300 trajectories were grouped into those that rebind on very short timescales ($\tau < 2$ ps), within 10 ps, and on timescales longer than 10 ps. The individually normalized probability distribution functions (pdfs) are shown in Figure S5. No NO migration to neighboring xenon-binding sites was observed on the 200 ps timescale because escape to the closest Xe site (Xe4), for example, occurs within 1 to 10 ns.[33,34]

Previous experimental and computational investigations[12,19,30,32,35–37] had found that the recombination kinetics of MbNO are non-exponential and involve two to three timescales, depending on the model used. The earliest reports reported timescales of 27.6 ps and 279.3 ps in a double-exponential fit.[12] Later, optical and IR experiments found short timescales ranging from 5 to 30 ps and longer timescales between 100 and 200 ps.[35–37] The experiments all agree on the existence of two sub-nanosecond timescales that differ by about one order of magnitude. Previous computations with reactive force fields typically found somewhat shorter rebinding times, between 5 ps and 20 ps,[19,32] depending on the asymptotic separation Δ.[38] The current simulations found multiple timescales in the 10 to 100 ps range that are in agreement with the optical and IR experiments. A more rapid component on the 1 to 2 ps timescale was also observed. The influence of Fe doming is clearly visible in the rebinding kinetics (see Figure 1). This results confirms that the force fields used here were of reasonable quality and allow to directly address a number of hypotheses.

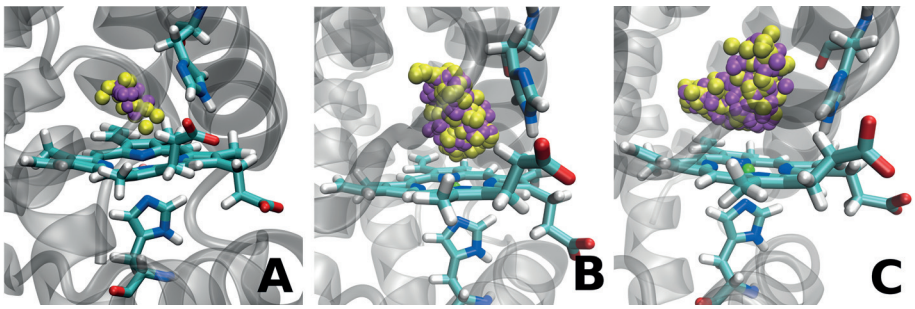

Figure 2. Typical trajectories for different rebinding timescales. NO positions are shown in yellow (N) and magenta (O). A) The picosecond process ($\tau = 1.6$ ps), B) the 10 picosecond process ($\tau = 42.1$ ps), and C) the 100 picosecond process ($\tau = 160.2$ ps).

First, direct connections with a recently proposed transient structure in the ^{2}A state can be made.

 © 2016 Wiley-VCH Verlag GmbH & Co. KGaA, Weinheim

Picosecond time-resolved[14] and XAS[5] experiments have suggested that the Fe-oop and the NO ligand motion are closely coupled. Interpretation of the experiments provided evidence for an Fe-oop, ligand-bound structure with a lifetime of 30 ± 10 ps. The present simulations on the ^{2}A PES alone indeed show the transient stabilization of such a state. The maximum lifetime was found to be 27 ps, and 41.7 % of the trajectories showed such a state (see Figure S3). Although they underestimate the experimentally determined lifetime of 30 ± 10 ps, the present simulations support the existence of such a state.

Another structurally elusive state that has been found for heme model compounds is the Fe–ON isomer.[21,39,40] Such a structure is sufficiently stabilized (by several kcal mol^{-1}) in NO-bound Mb, which should make it observable in IR experiments.[22] However, no such state has been found experimentally.[20] Simulations on the ^{2}A state alone show that the ligand is stabilized for tens of picoseconds in the Fe–ON state. However, when the reactive ^{2}A+^{4}A PES with a shift of $\Delta = -6.1$ kcal mol^{-1} (which best reproduces the DFT energies) is used, the Fe–ON configuration cannot be stabilized because in the region of the Fe–ON minimum, the repulsive ^{4}A state is lower in energy than the ^{2}A state. Hence, the ^{2}A minimum of the Fe–ON state is masked by the ^{4}A state and cannot be stabilized in wild-type Mb.

The asymptotic separation Δ depends on the chemical environment of the heme group. Hence, Δ changes when the environment is modified, for example, through amino acid mutation or embedding the heme group into a different protein. The effect of such changes can be quantified by simulations on the reactive ^2A+^4A PES with different Δ values. Reducing the asymptotic separation by 5 kcal mol^{-1} ($\Delta = -11.1$ kcal mol^{-1}) further destabilizes the Fe–ON state (Figure S6 A). For $\Delta = -6.1$ kcal mol^{-1} (Figure S6 B), the Fe–ON state is insignificantly sampled, and the system rebinds efficiently into the Fe–NO state. On the other hand, when the asymptotic separation is reduced to $\Delta = -1.1$ kcal mol^{-1} (Figure S6 C), the Fe–ON state is populated for extended periods of time during which spectroscopic characterization of this state should be possible. For comparison, a recent spectroscopic study found the dynamics of NO rebinding in Mb to be 2.5 times slower than in cytochrome c owing to the different active-site architectures.[41] According to transition-state theory, a factor of 2.5 corresponds to an energy difference of 0.5 kcal mol^{-1}. The thermodynamic stability of Mb upon mutation has been found to vary between -2 and $+6$ kcal mol^{-1},[42] which suggests that modifications in the active site can potentially stabilize the Fe–ON conformation through differential stabilization of the bound state relative to the unbound state.

With the coordinates from the reactive MD simulations, it is possible to provide a structural interpretation of the ca. 10 ps and 100 ps timescales found in the rebinding simulations. It is of particular interest to investigate in what respect the dynamics of these two states differ. Probability distribution functions of the a) NO ligand, b) all active-site residues, and c) all His64 side-chain atoms projected onto the heme plane are shown in Figure 3.

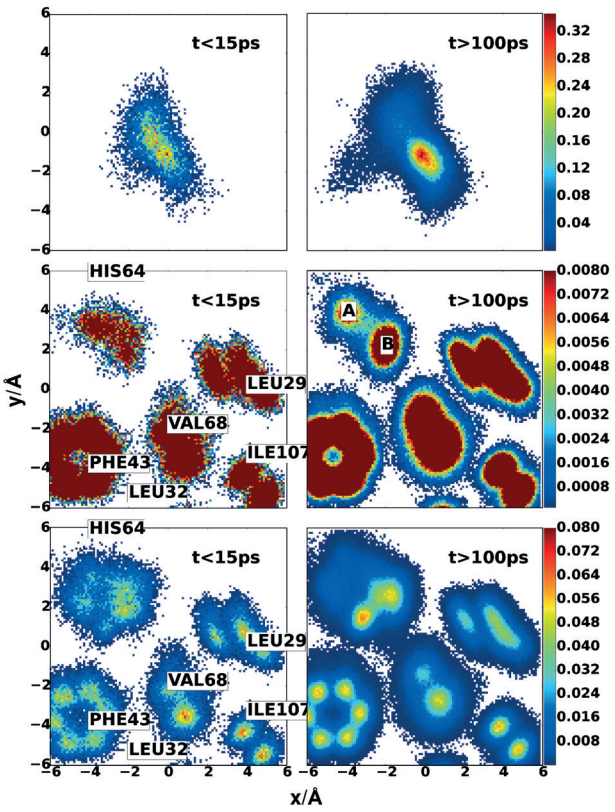

Figure 3. Top: The (*x*,*y*) probability distribution function for the rebinding of the free NO ligand on the $t < 15$ ps (left) and $t > 100$ ps (right) timescales. Middle: The (*x*,*y*) probability distribution functions for the NE2 atom of His64 on the two timescales. The two states for NE2 are labeled (A) and (B) and clearly distinguishable. Also shown are pdfs for all side-chain atoms of Phe43, Val68, Leu29, and Ile107. For Phe43, the phenyl ring is always parallel to the heme plane, and all six carbon atoms are clearly distinguishable. Bottom: As in the middle panel, but for the entire side chain of His64 and with different maximum heights of the pdfs.

The pdfs show that the NO ligand explores a much larger space for long rebinding times than for short rebinding times (Figure 3, top row). Furthermore, the NE2 atom of residue His64 occupies two clearly distinguishable states (A and B) in trajectories with long rebinding times, which are absent for rebinding within $\tau_1 = 10$ ps (Figure 3, middle row). The middle row emphasizes that for timescales τ_1, the His64 NE2 atom occupies space away from the iron center (located at (0,0)) whereas for longer timescales, the atom pushes in towards the heme iron by almost 2 Å, which hinders ligand rebinding. The estimated barriers, $\Delta G^{NE2}{\rightarrow} = 2.5$ kcal mol^{-1} for the forward and $\Delta G^{NE2}{\rightarrow} = 4.0$ kcal mol^{-1} for the reverse reaction, suggest that on the 100 ps timescale, state A is destabilized relative to state B. The corresponding barrier heights for the other His64 side-chain atoms range from 0.5 to 1.5 kcal mol^{-1}. Hence, on average, state B is separated from state A by a barrier of about 2 kcal mol^{-1}, with state B being lower in energy than state A.

The two states (A: green; B: red) are shown in Figure 4 together with the X-ray structure 1HJT[43] (gold). State A ("His64 out") is associated with the short rebinding timescale (10 ps) whereas state B ("His64 in") corresponds to the slow

 © 2016 Wiley-VCH Verlag GmbH & Co. KGaA, Weinheim

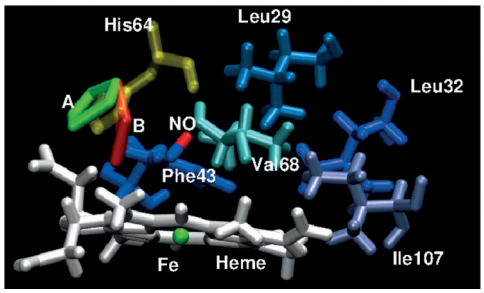

Figure 4. States A (green) and B (red) as found from the per-atom pdfs of the His64 side-chain atoms. The X-ray reference structure is shown in gold.

(100 ps) component. The barrier height corresponds to an interconversion time A⇄B on the sub-nanosecond timescale, which is supported by the explicit simulations and compares well with previous findings for CO-bound Mb with interconversion times of a few hundred picoseconds.[6,44]

For direct comparison with the XAS experiments, XANES spectra were computed (see the Supporting Information) for randomly selected MD-sampled structures with bound NO (40 structures), unbound NO within 3.5 Å of the heme Fe (20 structures), and unbound NO within 5.0 Å (10 structures). For the bound state, the computed spectrum ($I_b(E)$) agrees well with the experimental one up to 7.15 keV. For higher energies, the absorption signal is correctly described, but the computed intensity is too high (see Figure 5, top panel). The unbound structures yield $I_{ub,s}$ and $I_{ub,l}$ for the short and long Fe–NO separations, respectively, and nearly superimpose (Figure 5, inset) despite the different NO separations. Upon ligand photodissociation, the peak at 7.12 keV shifts to lower energy, and the intensity decreases between 7.12 and 7.15 keV and increases between 7.15 and 7.18 keV compared to the spectrum for the bound state. All of these features are consistent with previous experiments on MbNO and deoxy-Mb.[5,14]

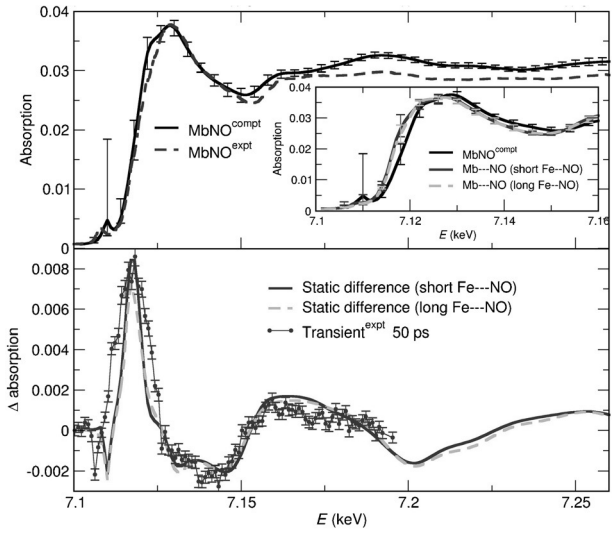

Figure 5. Top: Computed XANES spectrum for MbNO (black) compared to the experimental one (dashed). Vertical bars indicate the minimum and maximum absorption for all snapshots and are caused by conformational sampling. The inset compares computed spectra for MbNO and two sets of photodissociated systems (solid and dashed gray lines, see the main text). Bottom: Static difference spectra (solid and dashed gray lines) compared to the experimental transient at 50 ps (red).

The experimentally observed transient at 50 ps is compared with the averaged absorbance differences $\Delta I_{ub,s} = I_b - I_{ub,s}$ and $\Delta I_{ub,l} = I_b - I_{ub,l}$ in Figure 5. The two computed difference spectra are quite similar, except for slightly reduced amplitudes around 7.13 keV and 7.15 keV and an enhancement around 7.16 keV for $\Delta I_{ub,s}$ compared to $\Delta I_{ub,l}$ despite the two very different ligand positions. In both cases, the Fe-oop position ranges from 0.3 to 0.15 Å below the plane although for $\Delta I_{ub,s}$, positions closer to the in-plane position ($d = 0$) are also occupied. Compared to the experimental transient, $\Delta I_{ub,s}$ and $\Delta I_{ub,l}$ trace the major features but differ from it in the width of the 7.12 keV peak and the behavior between 7.13 and 7.15 keV. Figure S7 suggests that the presence or absence of photodissociated NO affects the XANES spectrum over the entire energy range from 7.10 to 7.15 keV and not just around 7.15 keV as previously assumed[5] because the signal also depends on the motion of the Fe atom relative to the heme plane. Within the signal-to-noise ratio of the experiment, it cannot be determined whether the ligand is close to the heme Fe or further away from it. It should be recalled that experimentally, a mixture of NO-bound and NO-unbound structures is measured because the photolysis yield is not 100%.

In conclusion, reactive MD simulations have given non-exponential kinetics for ligand rebinding. The determined timescales (10 and 100 ps) confirmed those from optical and IR experiments. The influence of the Fe-oop coordinate on the rebinding reaction has been directly established. The two timescales are associated with two structurally different states of the His64 side chain, "out" (state A) and "in" (state B), which control ligand access and rebinding dynamics. Although energetically accessible, the metastable ^{2}A Fe–ON state is likely to be unobservable in wild-type Mb because in this region of configurational space, the repulsive ^{4}A state is lower in energy, preventing stabilization. The present work supports a recently proposed, transient Fe-oop/NO-bound structure with a lifetime of up to 30 ps. The computed XAS spectra are in line with the experimentally recorded ones but are unable to distinguish between structures with photodissociated NO "close to" or "far away" from the heme Fe in the active site. The present work provides an atomistically refined picture and structural explanations and assignments for a range of experimental observations, which are all sensitive to the Fe-oop dynamics of NO after photodissociation in native Mb.

Acknowledgments

We acknowledge fruitful discussions with Chris Milne and helpful comments from Peter Hamm and Majed Chergui. This work was supported by the Swiss National Science Foundation through grant 200021-117810, and the NCCR MUST.

 © 2016 Wiley-VCH Verlag GmbH & Co. KGaA, Weinheim

Keywords: metastable states · myoglobin · nitric oxide · reactive molecular dynamics

How to cite: *Angew. Chem. Int. Ed.* **2016**, *55*, 10126–10130
Angew. Chem. **2016**, *128*, 10280–10285

[1] S. Fischer, K. W. Olsen, K. Nam, M. Karplus, *Proc. Natl. Acad. Sci. USA* **2011**, *108*, 5608–5613.
[2] J. G. Menting et al., *Proc. Natl. Acad. Sci.* **2014**, *111*, E3395–E3404.
[3] I. Schlichting, J. Berendzen, G. Phillips, R. Sweet, *Nature* **1994**, *371*, 808–812.
[4] F. Schotte, M. Lim, T. A. Jackson, A. V. Smirnov, J. Soman, J. S. Olson, G. N. Phillips, M. Wulff, P. A. Anfinrud, *Science* **2003**, *300*, 1944.
[5] M. Silatani, F. A. Lima, T. J. Penfold, J. Rittman, M. Reinhard, H. Rittmann-Frank, C. Borca, D. Grolimund, C. J. Milne, M. Chergui, *Proc. Natl. Acad. Sci. USA* **2015**, *112*, 12922–12927.
[6] K. A. Merchant, W. G. Noid, D. E. Thompson, R. Akiyama, R. F. Loring, M. D. Fayer, *J. Phys. Chem. B* **2003**, *107*, 4–7.
[7] J. Bredenbeck, J. Helbing, K. Nienhaus, G. U. Nienhaus, P. Hamm, *Proc. Natl. Acad. Sci. USA* **2007**, *104*, 14243–14248.
[8] P. Pacher, J. S. Beckman, L. Liaudet, *Physiol. Rev.* **2007**, *87*, 315–424.
[9] J. O. Lundberg et al., *Nat. Chem. Biol.* **2009**, *5*, 865–869.
[10] T. Traylor, V. Sharma, *Biochemistry* **1992**, *31*, 2847–2849.
[11] P. Cornelius, R. Hochstrasser, A. Steele, *J. Mol. Biol.* **1983**, *163*, 119–128.
[12] J. W. Petrich, J. C. Lambry, K. Kuczera, M. Karplus, C. Poyart, J. L. Martin, *Biochemistry* **1991**, *30*, 3975.
[13] D. Ionascu, F. Gruia, X. Ye, A. Yu, F. Rosca, C. B. A. Demidov, J. S. Olson, P. M. Champion, *J. Am. Chem. Soc.* **2005**, *127*, 16921–16934.
[14] S. G. Kruglik, B.-K. Yoo, S. Franzen, M. H. Vos, J.-L. Martin, M. Negrerie, *Proc. Natl. Acad. Sci. USA* **2010**, *107*, 13678.
[15] J. Kim, J. Park, T. Lee, M. Lim, *J. Phys. Chem. B* **2012**, *116*, 13663–13671.
[16] B.-K. Yoo, S. G. Kruglik, I. Lamarre, J.-L. Martin, M. Negrerie, *J. Phys. Chem. B* **2012**, *116*, 4106–4114.
[17] S. Kim, G. Jin, M. Lim, *J. Phys. Chem. B* **2004**, *108*, 20366.
[18] D. R. Nutt, M. Meuwly, *Biophys. J.* **2006**, *90*, 1191.
[19] J. Danielsson, M. Meuwly, *J. Chem. Theory Comput.* **2008**, *4*, 1083.
[20] K. Nienhaus, P. Palladino, G. U. Nienhaus, *Biochemistry* **2008**, *47*, 935.
[21] N. Xu, J. Yi, G. B. Richter-Addo, *Inorg. Chem.* **2010**, *49*, 6253–6266.
[22] D. R. Nutt, M. Karplus, M. Meuwly, *J. Phys. Chem. B* **2005**, *109*, 21118.
[23] D. R. Nutt, M. Meuwly, *Proc. Natl. Acad. Sci. USA* **2004**, *101*, 5998.
[24] M. W. Lee, J. K. Carr, M. Göllner, P. Hamm, M. Meuwly, *J. Chem. Phys.* **2013**, *139*, 054506.
[25] M. Soloviov, M. Meuwly, *J. Chem. Phys.* **2015**, *143*, 105103.
[26] N. Aronszajn, *Trans. Am. Math. Soc.* **1950**, *68*, 337.
[27] T. Hollebeek, T. S. Ho, H. Rabitz, *Annu. Rev. Phys. Chem.* **1999**, *50*, 537.
[28] T. S. Ho, H. Rabitz, *J. Chem. Phys.* **1996**, *104*, 2584.
[29] M. Meuwly, J. M. Hutson, *J. Chem. Phys.* **1999**, *110*, 8338.
[30] M. Meuwly, O. M. Becker, R. Stote, M. Karplus, *Biophys. Chem.* **2002**, *98*, 183–207.
[31] M. Lim, T. A. Jackson, P. A. Anfinrud, *Proc. Natl. Acad. Sci. USA* **1993**, *90*, 5801.
[32] D. R. Nutt, M. Meuwly, *Biophys. J.* **2006**, *90*, 1191–1201.
[33] C. Bossa, M. Anselmi, D. Roccatano, A. Amadei, B. Vallone, M. Brunori, A. Di Nola, *Biophys. J.* **2004**, *86*, 3855.
[34] N. Plattner, M. Meuwly, *Biophys. J.* **2012**, *102*, 333.
[35] Y. Kholodenko, E. Gooding, Y. Dou, M. Ikeda-Saito, R. Hochstrasser, *Biochemistry* **1999**, *38*, 5918–5924.
[36] X. Ye, A. Demidov, P. Champion, *J. Am. Chem. Soc.* **2002**, *124*, 5914–5924.
[37] S. Kim, G. Jin, M. Lim, *J. Phys. Chem. B* **2004**, *108*, 20366–20375.
[38] P. Banushkina, M. Meuwly, *J. Chem. Phys.* **2007**, *127*, 135101.
[39] M. Carducci, M. Pressprich, P. Coppens, *J. Am. Chem. Soc.* **1997**, *119*, 2669–2678.
[40] L. Cheng, I. Novozhilova, C. Kim, A. Kovalevsky, K. A. Bagley, P. Coppens, G. B. Richter-Addo, *J. Am. Chem. Soc.* **2000**, *122*, 7142.
[41] N. T. Hunt, G. M. Greetham, M. Towrie, A. W. Parker, N. P. Tucker, *Biochem. J.* **2011**, *433*, 459–468.
[42] K. P. Kepp, *Biochim. Biophys. Acta Proteins Proteomics* **2015**, *1854*, 1239–1248.
[43] E. A. Brucker, J. S. Olson, M. Ikeda-Saito, G. N. Phillips, *Prot. Struct. Funct. Genet.* **1998**, *30*, 352.
[44] J. Ma, S. Huo, J. Straub, *J. Am. Chem. Soc.* **1997**, *119*, 2541–2551.

Received: May 11, 2016
Published online: July 13, 2016

 © 2016 Wiley-VCH Verlag GmbH & Co. KGaA, Weinheim